

# Faddeev-Yakubovsky calculations for light $\Lambda\Lambda$ hypernuclei

I.N. Filikhin<sup>a</sup>, A. Gal<sup>a</sup>

<sup>a</sup>Racah Institute of Physics, The Hebrew University, Jerusalem 91904, Israel

## Abstract

New Faddeev-Yakubovsky calculations are reported for  ${}_{\Lambda\Lambda}^6\text{He}$  and  ${}_{\Lambda\Lambda}^{10}\text{Be}$  in terms of clusters of  $\alpha$ 's and  $\Lambda$ 's, using  $\Lambda\Lambda$   $s$ -wave potentials motivated by several of the Nijmegen model interactions. The self consistency of the  $\Lambda\Lambda$  hypernuclear world data for these species is discussed. The newly reported  ${}_{\Lambda\Lambda}^6\text{He}$  event is found to be compatible with  $\Lambda\Lambda$  interaction strengths provided by the Nijmegen soft-core one-boson-exchange model NSC97. Faddeev calculations for  ${}_{\Lambda\Lambda}^5\text{H}$  and  ${}_{\Lambda\Lambda}^5\text{He}$  suggest that these  $\Lambda\Lambda$  hypernuclei are stable against emitting  $\Lambda$ 's for any (essentially attractive)  $\Lambda\Lambda$  interaction, whereas calculations for  ${}_{\Lambda\Lambda}^4\text{H}$  do not allow a clear-cut conclusion whether or not it is particle stable.

*PACS:* 21.80.+a, 11.80.Jy, 21.45.+v

*Keywords:*  $\Lambda\Lambda$  hypernuclei;  $\Lambda\Lambda$  interaction; Faddeev-Yakubovsky equations; Few-body systems.

Corresponding author: Avraham Gal

Tel: +972 2 6584930, Fax: +972 2 5611519

E mail: avragal@vms.huji.ac.il

(October 29, 2018)

## I. INTRODUCTION

Data on strangeness  $S = -2$  hypernuclear systems is rather scarce, and no data exist for systems with higher strangeness content of hyperons ( $Y$ ). Multistrange hadronic matter in finite systems and in bulk is predicted on general grounds to be stable, up to strangeness violating weak decays (see Ref. [1] for a recent review). Until recently only three candidates existed for  $\Lambda\Lambda$  hypernuclei which fit events seen in emulsion experiments [2–4]. The  $\Lambda\Lambda$  binding energies deduced from these events indicated that the  $\Lambda\Lambda$  interaction is strongly attractive in the  $^1S_0$  channel [5,6], although it had been realized [7,8] that the binding energies of the two older events,  ${}_{\Lambda\Lambda}^6\text{He}$  and  ${}_{\Lambda\Lambda}^{10}\text{Be}$ , are inconsistent with each other. This outlook is perhaps undergoing an important change following the very recent report from the KEK hybrid-emulsion experiment E373 on a new candidate [9] for  ${}_{\Lambda\Lambda}^6\text{He}$ , with binding energy substantially lower than that deduced from the older event [3]. Furthermore, there are also indications from the AGS experiment E906 for the production of light  $\Lambda\Lambda$  hypernuclei [10], perhaps as light even as  ${}_{\Lambda\Lambda}^4\text{H}$ , in the  $(K^-, K^+)$  reaction on  ${}^9\text{Be}$ .

The study of multistrange systems can provide rather stringent tests of microscopic models for the baryon-baryon interaction. Over the years, the Nijmegen group has constructed a number of one-boson-exchange (OBE) models for the baryon-baryon interaction ( $NN$ ,  $\Lambda N - \Sigma N$ , and  $\Xi N - \Lambda\Lambda - \Sigma\Sigma - \Lambda\Sigma$ ) using SU(3)-flavor symmetry to relate baryon-baryon-meson coupling constants and phenomenological hard or soft cores at short distances (for a recent review, see Ref. [11]). In addition, the Jülich group has constructed OBE models for the  $YN$  interaction along the lines of the Bonn Model for the  $NN$  interaction, using SU(6) symmetry to relate coupling constants and short-range form factors [12]. The SU(6) quark model has also been used to derive baryon-baryon interactions within a unified framework of a  $(3q) - (3q)$  resonating group method, augmented by a few effective meson exchange potentials of scalar and pseudoscalar meson nonets directly coupled to quarks [13]. In all of these rather different baryon-baryon interaction models only 35  $YN$  low-energy, generally imprecise data points serve for the purpose of steering phenomenologically the extrapolation from the  $NN$  sector, which relies on thousands of data points, into the strange  $YN$  and  $YY$  sectors. It is therefore of utmost importance to confront these models with the new  $\Lambda\Lambda$  hypernuclear data in order to provide meaningful constraints on the extrapolation to  $S = -2$  and beyond.

In this paper we report on Faddeev-Yakubovsky three-body and four-body calculations of light  $\Lambda\Lambda$  hypernuclei, using  $\Lambda\Lambda$   $s$ -wave potentials which simulate the low-energy  $s$ -wave scattering parameters produced by several Nijmegen OBE models. Our own work is compared to other recent variational calculations [14–16]. The advantage of the Faddeev-Yakubovsky method is that it accounts properly for *all* the relevant rearrangement channels. The purpose of our calculations is twofold: to check the self consistency of the data, particularly for  ${}_{\Lambda\Lambda}^6\text{He}$  and  ${}_{\Lambda\Lambda}^{10}\text{Be}$  [17] which are treated here as clusters of  $\alpha$ 's and  $\Lambda$ 's; and to find out which of the recent Nijmegen Soft-Core (NSC97) models [18,19], or the Extended Soft-Core (ESC00) interaction model [11], is the most appropriate one for describing well  $\Lambda\Lambda$  hypernuclei. The paper is organized as follows. The Faddeev-Yakubovsky approach, its restriction to  $s$  waves for light hypernuclei, and some computational aspects are described briefly in Sect. II. We specify the input potentials, fitting as much as possible known binding energies of given hypernuclear subsystems. The results of our Faddeev-Yakubovsky calculations for

${}_{\Lambda\Lambda}^6\text{He}$  and  ${}_{\Lambda\Lambda}^{10}\text{Be}$  in terms of clusters of  $\alpha$ 's and  $\Lambda$ 's, using  $\Lambda\Lambda$   $s$ -wave potentials motivated by several Nijmegen model interactions, are reported and discussed in Sect. III. Faddeev calculations for  ${}_{\Lambda\Lambda}^5\text{H}$  and  ${}_{\Lambda\Lambda}^5\text{He}$  are also reported. A preliminary, partial report of these results has just appeared as a Rapid Communication [20]. In the Summary section we briefly discuss the implications of our work on the stability of  ${}_{\Lambda\Lambda}^4\text{H}$ , for which our Faddeev-Yakubovsky calculations at present are in progress.

## II. METHODOLOGY

### A. Faddeev equations

The bound states of the three-body systems considered in this work are obtained by solving the differential Faddeev equations [21]

$$(H_0 + V_\beta^c + V_\beta^s - E)U_\beta = -V_\beta^s \sum_{\gamma=1, \gamma \neq \beta}^3 U_\gamma, \quad \beta = 1, 2, 3, \quad (1)$$

where  $V_\beta^c$  and  $V_\beta^s$  are Coulomb and short-range pairwise interactions respectively in the channel  $\beta$ ,  $H_0$  is the kinetic energy operator,  $E$  is the total energy and the wavefunction of the three-body system is given as a sum over the three Faddeev components,  $\Psi = \sum_{\beta=1}^3 U_\beta$ , corresponding to the two-body breakup channels. The Faddeev components are functions of spin-isospin variables and of relative Jacobi coordinates. When two constituents of the three-body system are identical, for example  $\Lambda$  hyperons in  ${}_{\Lambda\Lambda}^6\text{He}$  ( $\alpha\Lambda\Lambda$ ) generically of the form  $C\Lambda\Lambda$  ( $C = \text{core}$ ), the coupled set of Faddeev equations simplifies as follows:

$$(H_0 + V_{\Lambda\Lambda} - E)U = -V_{\Lambda\Lambda}(W - P_{23}W), \quad (H_0 + V_{\Lambda C} - E)W = -V_{\Lambda C}(U - P_{23}W), \quad (2)$$

where  $P_{23}$  is the permutation operator for the  $\Lambda$  hyperons (particles 2,3).  $U$  is the Faddeev component corresponding to the rearrangement channel  $\alpha - (\Lambda\Lambda)$  and  $W$  corresponds to the rearrangement channel  $(\alpha\Lambda) - \Lambda$ :

$$\Psi_{\alpha-(\Lambda\Lambda)} = U, \quad \Psi_{(\alpha\Lambda)-\Lambda} = (1 - P_{23})W; \quad \Psi = \Psi_{\alpha-(\Lambda\Lambda)} + \Psi_{(\alpha\Lambda)-\Lambda}. \quad (3)$$

The probability weights for the various rearrangement channels  $\beta$  in the total wavefunction  $\Psi$  of  ${}_{\Lambda\Lambda}^6\text{He}$  are defined by

$$P_\beta = \frac{\langle \Psi, \Psi_\beta \rangle}{\langle \Psi, \Psi \rangle}. \quad (4)$$

For  ${}^9_\Lambda\text{Be}$ , here considered as a  $\Lambda\alpha\alpha$  system, a similar simplification occurs, but where the minus sign in Eqs. (2) in front of  $P_{23}$  arising from the Fermi-Dirac statistics for the  $\Lambda$ 's is replaced by a plus sign owing to the Bose-Einstein statistics for the  $\alpha$ 's, and  $V^c$  is added on the l.h.s. of the first Faddeev equation. These Faddeev equations, for  ${}^9_\Lambda\text{Be}(\frac{1}{2}^+)$  and  ${}_{\Lambda\Lambda}^6\text{He}(0^+)$  ground states, were solved in Ref. [22] using an  $s$ -wave approximation in which only the  $\ell_\alpha = 0$ ,  $\lambda_\alpha = 0$  partial waves were retained for the Jacobi-coordinate  $\mathbf{x}_\alpha$ ,  $\mathbf{y}_\alpha$  degrees of freedom, respectively, where

$$\mathbf{x}_\alpha = \mathbf{r}_\beta - \mathbf{r}_\gamma, \quad \mathbf{y}_\alpha = \frac{m_\beta \mathbf{r}_\beta + m_\gamma \mathbf{r}_\gamma}{m_\beta + m_\gamma} - \mathbf{r}_\alpha, \quad \beta > \gamma \neq \alpha, \quad \alpha, \beta, \gamma = 1, 2, 3, \quad (5)$$

where  $m_\alpha$  and  $\mathbf{r}_\alpha$ ,  $\alpha=1,2,3$ , are the mass and the position vector of the  $\alpha$ -th constituent, respectively. (The total orbital angular momentum is given here by  $\mathbf{L} = \vec{\ell}_\alpha + \vec{\lambda}_\alpha$ ). The present calculation extends and updates the previous one. We comment in Sections III and IV on the validity of the  $s$ -wave approximation.

Other three-body systems studied in the present work are the isodoublet  ${}_{\Lambda\Lambda}^5\text{H}$ ,  ${}_{\Lambda\Lambda}^5\text{He}$  charge-symmetric hypernuclei, here considered as  ${}^3\text{H}\Lambda\Lambda$  and  ${}^3\text{He}\Lambda\Lambda$  respectively. For the ground state ( $\frac{1}{2}^+$ ) of this system, the  $s$ -wave Faddeev equations assume the form

$$\begin{aligned} (H_0^u(x_1, y_1) + v_{\Lambda\Lambda}^s(x_1) - E)\mathcal{U}(x_1, y_1) &= -v_{\Lambda\Lambda}^s(x_1) \int_{-1}^1 dv_1 \frac{x_1 y_1}{x'_1 y'_1} A \mathcal{W}(x'_1, y'_1), \\ (H_0^w(x_2, y_2) + V_{\Lambda C}(x_2) - E)\mathcal{W}(x_2, y_2) &= -\frac{1}{2} V_{\Lambda C}(x_2) \left[ \int_{-1}^1 dv_2 \frac{x_2 y_2}{x'_2 y'_2} A^T \mathcal{U}(x'_2, y'_2) \right. \\ &\quad \left. + \int_{-1}^1 dv_2 \frac{x_2 y_2}{x''_2 y''_2} B \mathcal{W}(x''_2, y''_2) \right], \end{aligned} \quad (6)$$

where  $v_{\Lambda\Lambda}^s(x)$  is the singlet  $\Lambda\Lambda$  potential,  $V_{\Lambda C} = \text{diag}\{v_{\Lambda C}^s, v_{\Lambda C}^t\}$  with  $v_{\Lambda C}^s$  and  $v_{\Lambda C}^t$  the singlet and triplet  $\Lambda C$  interaction potentials, respectively,

$$\begin{aligned} H_0^u(x, y) &= -\frac{\hbar^2}{2M_1} \partial_y^2 - \frac{\hbar^2}{2\mu_1} \partial_x^2, & H_0^w(x, y) &= -\frac{\hbar^2}{2M_2} \partial_y^2 - \frac{\hbar^2}{2\mu_2} \partial_x^2, \\ A &= \left(-\frac{1}{2}, -\frac{\sqrt{3}}{2}\right), & B &= \left(\frac{-\frac{1}{2}}{\frac{\sqrt{3}}{2}}, \frac{\frac{\sqrt{3}}{2}}{\frac{1}{2}}\right), \\ \mathcal{W}(x, y) &= (\mathcal{W}^s(x, y), \mathcal{W}^t(x, y))^T. \end{aligned}$$

The appropriate reduced masses are given by

$$M_1 = 2 \frac{m_C m_\Lambda}{m_C + 2m_\Lambda}, \quad M_2 = \frac{m_\Lambda (m_C + m_\Lambda)}{m_C + 2m_\Lambda}, \quad \mu_1 = \frac{m_\Lambda}{2}, \quad \mu_2 = \frac{m_C m_\Lambda}{m_C + m_\Lambda}.$$

The appropriate transformation of coordinates is given by

$$\begin{aligned} x'_1 &= \left(\left(\frac{\mu_1}{m_\Lambda} x_1\right)^2 + y_1^2 + 2\frac{\mu_1}{m_\Lambda} x_1 y_1 v_1\right)^{1/2}, & y'_1 &= \frac{m_C}{m_C + m_\Lambda} \left(\left(\frac{m_\Lambda}{M_1} x_1\right)^2 + y_1^2 - 2\frac{m_\Lambda}{M_1} x_1 y_1 v_1\right)^{1/2}, \\ x''_1 &= \left(\left(\frac{\mu_1}{m_\Lambda} x_1\right)^2 + y_1^2 - 2\frac{\mu_1}{m_\Lambda} x_1 y_1 v_1\right)^{1/2}, & y''_1 &= \frac{m_C}{m_C + m_\Lambda} \left(\left(\frac{m_\Lambda}{M_1} x_1\right)^2 + y_1^2 + 2\frac{m_\Lambda}{M_1} x_1 y_1 v_1\right)^{1/2}, \\ x'_2 &= \left(\left(\frac{\mu_2}{m_\Lambda} x_2\right)^2 + y_2^2 + 2\frac{\mu_2}{m_\Lambda} x_2 y_2 v_2\right)^{1/2}, & y'_2 &= \frac{1}{2} \left(\left(\frac{m_\Lambda}{M_2} x_2\right)^2 + y_2^2 - 2\frac{m_\Lambda}{M_2} x_2 y_2 v_2\right)^{1/2}, \\ x''_2 &= \left(\left(\frac{\mu_2}{m_C} x_2\right)^2 + y_2^2 - 2\frac{\mu_2}{m_C} x_2 y_2 v_2\right)^{1/2}, & y''_2 &= \frac{m_\Lambda}{m_C + m_\Lambda} \left(\left(\frac{m_C}{M_2} x_2\right)^2 + y_2^2 + 2\frac{m_C}{M_2} x_2 y_2 v_2\right)^{1/2}. \end{aligned}$$

Here  $v_j$  is the cosine of angle between  $\mathbf{x}_j$  and  $\mathbf{y}_j$ . The  $s$ -wave total wavefunction then assumes the form

$$\Psi(x_1, y_1, v_1) = \mathcal{U}(x_1, y_1)/(x_1 y_1) + A\mathcal{W}(x'_1, y'_1)/(x'_1 y'_1) + A\mathcal{W}(x''_1, y''_1)/(x''_1 y''_1) \quad , \quad (7)$$

where the product  $A\mathcal{W}$  ensures that the two  $\Lambda$ 's are in a  $^1S_0$  state as required by the Pauli principle. Note that the squares of elements of  $A$  correspond then to a  $(2J+1)$  average over the  $J=0,1$  (singlet and triplet, respectively)  $^4_\Lambda\text{H}$  and  $^4_\Lambda\text{He}$  states. We also note in passing that the  $s$ -wave Faddeev equations for  $^6_{\Lambda\Lambda}\text{He}$  ( $\alpha\Lambda\Lambda$ ) and for  $^9_\Lambda\text{Be}$  ( $\Lambda\alpha\alpha$ ) are obtained from Eqs. (6) by setting  $A=B=1$  with obvious changes in the notation for the masses and the total wavefunction (and adding the Coulomb potential between the two  $\alpha$ 's in  $^9_\Lambda\text{Be}$ ).

## B. Yakubovsky equations

The four-particle wavefunction  $\Psi$  is decomposed, in the Faddeev-Yakubovsky method [21], into components which are in a one to one correspondence with all chains of partitions. The chains consist of two-cluster partitions  $a_2$  (e.g.,  $(ijk)l$  or  $(ij)(kl)$ ) and three-cluster partitions  $a_3$  (e.g.,  $(ij)kl$ ) obeying the relation  $a_3 \subset a_2$ . The latter means that the partition  $a_3$  can be obtained from the partition  $a_2$  by splitting up one subsystem. Any three-cluster partition  $a_3$  may be obtained in this way from three different two-cluster partitions  $b_2$ ,  $c_2$  and  $d_2$ . It is easy to see that there exist generally 18 chains of partitions for a four-particle system. The components  $\Psi_{a_3 a_2}$  obey the differential Yakubovsky equations [23]

$$(H_0 + V_{a_3} - E)\Psi_{a_3 a_2} + V_{a_3} \sum_{(c_3 \neq a_3)} \Psi_{c_3 a_2} = -V_{a_3} \sum_{d_2 \neq a_2} \sum_{(d_3 \neq a_3) \subset a_2} \Psi_{d_3 d_2} \quad . \quad (8)$$

Here  $H_0$  is the kinetic-energy operator and  $V_{a_3}$  stands for the two-body potential acting within the two-particle subsystem of a partition  $a_3$  (e.g.,  $V_{a_3} = V_{ij}$  with  $a_3 = (ij)kl$ ).

We demonstrate the Yakubovsky equations for the case of two pairs, each consisting of identical constituents. To be more specific we consider the pair (1,2) to consist of two identical fermions, and the pair (3,4) to consist of two identical bosons, altogether simulating the four-body  $\Lambda\Lambda\alpha\alpha$  system. This results in a reduction of the number of Faddeev-Yakubovsky components into seven independent components satisfying the following Yakubovsky differential equations:

$$(H_0 + V^c + V_{\alpha\alpha} - E)U_1 + V_{\alpha\alpha}(I + P_{34})U_2 = -V_{\alpha\alpha}((I + P_{34})U_4 - P_{12}(I + P_{34})W_3) \quad , \quad (9)$$

$$(H_0 + V^c + V_{\Lambda\alpha} - E)U_2 + V_{\Lambda\alpha}(U_1 + P_{34}U_2) = -V_{\Lambda\alpha}(P_{34}U_4 - P_{12}U_1 + W_2 - P_{12}W_3) \quad , \quad (10)$$

$$(H_0 + V^c + V_{\Lambda\Lambda} - E)U_3 + V_{\Lambda\Lambda}(I - P_{12})U_4 = -V_{\Lambda\Lambda}((I - P_{12})U_2 + (I - P_{12})P_{34}W_3) \quad , \quad (11)$$

$$(H_0 + V^c + V_{\Lambda\alpha} - E)U_4 + V_{\Lambda\alpha}(U_3 - P_{12}U_4) = -V_{\Lambda\alpha}(P_{34}U_3 - P_{12}U_2 + W_1 + P_{34}W_3) \quad , \quad (12)$$

$$(H_0 + V^c + V_{\Lambda\Lambda} - E)W_1 + V_{\Lambda\Lambda}W_2 = -V_{\Lambda\Lambda}(I - P_{12})U_1 \quad , \quad (13)$$

$$(H_0 + V^c + V_{\alpha\alpha} - E)W_2 + V_{\alpha\alpha}W_1 = -V_{\alpha\alpha}(I + P_{34})U_3, \quad (14)$$

$$(H_0 + V^c + V_{\Lambda\alpha} - E)W_3 - V_{\Lambda\alpha}P_{12}P_{34}W_3 = -V_{\Lambda\alpha}(U_4 + U_2), \quad (15)$$

where  $U_\beta$  ( $\beta=1,2,3,4$ ) are Yakubovsky components corresponding to three-cluster partitions evolving from 3+1 type breakup into two-cluster partitions,  $W_\gamma$  ( $\gamma=1,2,3$ ) are Yakubovsky components corresponding to three-cluster partitions evolving from 2+2 type breakup into two-cluster partitions:

$$U_1 = \Psi_{(34)2,1}, \quad U_2 = \Psi_{(24)3,1}, \quad U_3 = \Psi_{(12)4,3}, \quad U_4 = \Psi_{(24)1,3}, \quad (16)$$

$$W_1 = \Psi_{(12),34}, \quad W_2 = \Psi_{(34),12}, \quad W_3 = \Psi_{(13),24}, \quad (17)$$

in the shorthand notation of Ref. [24] for the  $(a_3, a_2)$  chains of partitions. For each Yakubovsky component the natural Jacobi relative coordinates are employed. For the particular  $\Lambda\Lambda\alpha\alpha$  problem under consideration,  $V^c$  stands for the Coulomb interaction between particles 3 and 4, expressed in terms of the corresponding Jacobi coordinates. There are four rearrangement channels altogether, defined in terms of the following wavefunctions:

$$\Psi_{(\alpha\alpha\Lambda)\Lambda} = (I - P_{12})U_1 + (I + P_{34} - P_{12}P_{34} - P_{12})U_2, \quad (18)$$

$$\Psi_{(\alpha\Lambda\Lambda)\alpha} = (I + P_{34})U_3 + (I + P_{34} - P_{12}P_{34} - P_{12})U_4, \quad (19)$$

$$\Psi_{(\alpha\alpha)(\Lambda\Lambda)} = W_1 + W_2, \quad \Psi_{(\alpha\Lambda)(\alpha\Lambda)} = (I + P_{34} - P_{12}P_{34} - P_{12})W_3. \quad (20)$$

The total wavefunction can be written as

$$\Psi = \Psi_{(\alpha\alpha\Lambda)\Lambda} + \Psi_{(\alpha\Lambda\Lambda)\alpha} + \Psi_{(\alpha\alpha)(\Lambda\Lambda)} + \Psi_{(\alpha\Lambda)(\alpha\Lambda)}. \quad (21)$$

The probability weights for the various rearrangement channels  $\beta$  in the total wavefunction of  ${}^{10}_{\Lambda\Lambda}\text{Be}$  are given by Eq. (4) of the previous subsection.

### C. Computation

The  $s$ -wave Faddeev-Yakubovsky equations are solved using the cluster reduction method (CRM) which was developed by Yakovlev and Filikhin [25] and has been recently applied to calculate bound states and low-energy scattering for systems of three and four nucleons [26]. In this method, the Faddeev-Yakubovsky components are decomposed in terms of the eigenfunctions of the Hamiltonians of the two- or three-particle subsystems. Due to the projection onto elements of an orthogonal basis, one obtains a set of equations with effective interactions corresponding to the relative motion of the various clusters. Thus, the Faddeev components  $\mathcal{U}_\alpha$ ,  $\alpha=1,2,3$  are written in the following form:

$$\mathcal{U}_\alpha(x, y) = \sum_{l=0}^{\infty} \phi_{\alpha,l}(x) f_{\alpha,l}(y). \quad (22)$$

Here, the basic functions  $\phi_{\alpha,l}$  are the solutions of the two-body Schrödinger equation for the subsystem  $\alpha$ :

$$\left(-\frac{\hbar^2}{2\mu_\alpha}\partial_x^2 + v_\alpha(x)\right)\phi_{\alpha,l}(x) = \varepsilon_{\alpha,l}\phi_{\alpha,l}(x) , \quad \phi_{\alpha,l}(0) = \phi_{\alpha,l}(R_{\text{cutoff}}) = 0 , \quad (23)$$

where  $\mu_\alpha$  is the reduced mass of the subsystem  $\alpha$ , and  $v_\alpha(x)$  is the  $s$ -wave projected potential  $V_\alpha$ . Substituting (22) into (1) and projecting onto the orthogonal basis  $\phi_{\alpha,l}(x)$  one obtains a set of integro-differential equations for the functions  $f_{\alpha,l}(y)$ . A fairly small number of terms is sufficient, using limited computer resources [26], to generate a stable and precise numerical solution independently of the value adopted for  $R_{\text{cutoff}}$ , provided the latter was chosen sufficiently large. The convergence of a typical  ${}_{\Lambda\Lambda}{}^6\text{He}$  Faddeev calculation, and of a typical  ${}_{\Lambda\Lambda}{}^{10}\text{Be}$  Yakubovsky calculation, as function of the number of terms  $N$  retained in Eq. (22) above is demonstrated in Fig. 1. Such calculations usually require less than 10 terms to reach good convergence. The CRM has been recently used by one of us to study  ${}^3_\Lambda\text{H}$  as a three-body  $pn\Lambda$  system [27], and  ${}^9_\Lambda\text{Be}$  and  ${}_{\Lambda\Lambda}{}^6\text{He}$  in terms of three-cluster systems  $\Lambda\alpha\alpha$  and  $\alpha\Lambda\Lambda$ , respectively [22]. Here we update and extend that calculation, while applying the CRM for the first time to the solution of the  $\alpha\alpha\Lambda\Lambda$  four-body problem in terms of Yakubovsky equations.

#### D. Potentials

The  $\Lambda\Lambda$  interaction potentials in the  ${}^1S_0$  channel which are used as input to the Faddeev equations are of the three-range Gaussian form

$$V_{\Lambda\Lambda} = \sum_i^3 v^{(i)} \exp(-r^2/\beta_i^2) , \quad (24)$$

following the work of Hiyama *et al.* [14] where a phase-equivalent  $\Lambda\Lambda$  potential of this soft-core form was fitted to the Nijmegen model D (ND) hard-core interaction [28] assuming the same hard core for the  $NN$  and  $\Lambda\Lambda$  potentials in the  ${}^1S_0$  channel. Our simulation of the ND interaction potential is specified, for  $\gamma = 1$ , in Table I. For other interactions we have renormalized the strength of the medium-range attractive component ( $i = 2$ ) of this potential such that, using values of  $\gamma \neq 1$ , it yields values for the scattering length and for the effective range as close to values prescribed by us. In Table II we list the low-energy parameters for several Nijmegen potentials, particularly the soft-core NSC97 model  $\Lambda\Lambda$  potentials [19], and in parentheses the corresponding values for potentials of the form (24) using the listed values of  $\gamma$ . Three of these fitted  ${}^1S_0$  potentials are shown in Fig. 2. The strongest  $\Lambda\Lambda$  potential is the one with the largest absolute value of scattering length, due to the ESC00 model [11], and the weakest one is associated with the smallest absolute value of scattering length, due to one of the NSC97 model potentials. The difference between the various NSC97 potentials (a)-(f) is of second order, all of them being only fairly weakly attractive.

The  $\alpha\alpha$  short-range interaction and the  $\Lambda\alpha$  interaction are given in terms of two-range Gaussian (Isle) potentials

$$V^{(j)} = V_{\text{rep}}^{(j)} \exp(-r^2/\beta_{\text{rep}}^{(j)^2}) - V_{\text{att}}^{(j)} \exp(-r^2/\beta_{\text{att}}^{(j)^2}) , \quad (25)$$

where the superscript  $j$  specifies the interacting system. For the  $\alpha\alpha$  short-range interaction potential we used the  $s$ -wave component of the Ali-Bodmer potential [29]. A Comment about the validity of using this phenomenological potential, which does not reflect at short  $\alpha\alpha$  distance the underlying inner structure of the  $\alpha$  clusters, is made below in Sect. III. The  $\Lambda\alpha$  interaction potential is due to Ref. [30] where the binding energy and mesonic weak decay of  ${}^5_{\Lambda}\text{He}$  were studied. The resulting  $\Lambda$ -hyperon density distribution has been shown very recently [31] to closely resemble that due to a microscopic calculation of  ${}^5_{\Lambda}\text{He}$  using  $YN$  interactions which simulate those of model NSC97 [18]. The parameters of these potentials are listed in Table III. Similar potentials were constructed by us for the  $\Lambda-{}^3\text{H}$  and  $\Lambda-{}^3\text{He}$  singlet and triplet interactions by refitting the range parameter  $\beta_{\text{rep}}$  of the  $\Lambda\alpha$  Isle potential (25) to reproduce the known binding energies of  ${}^4_{\Lambda}\text{H}$  and  ${}^4_{\Lambda}\text{He}$ , respectively. These fitted range parameters and the binding energies calculated using this procedure are shown in Table IV, in comparison with the experimentally known values [32,33]. The  ${}^9_{\Lambda}\text{Be}$  calculation is discussed below in the next section.

### III. RESULTS AND DISCUSSION

We first applied the  $\alpha\alpha$  and  $\Lambda\alpha$  potentials, specified by Eq. (25) and in Table III, to the solution of the  $s$ -wave Faddeev equations for the  $\alpha\alpha\Lambda$  system. The calculated ground-state binding energy of  ${}^9_{\Lambda}\text{Be}$  in this three-body model is given in Table IV and is in close agreement with the measured  $B_{\Lambda}$  value, with no need for renormalization or for introducing three-body interactions. Had we used a purely attractive  $\Lambda\alpha$  interaction potential such as the single-Gaussian form due to Bando *et al.* [34], the calculated ground-state binding energy of  ${}^9_{\Lambda}\text{Be}$  would have come out too low by about 1 MeV [22]. On the other hand the calculations by Motoba *et al.* [35], using an Isle potential (similar to ours) for the  $\Lambda\alpha$  interaction, overbind  ${}^9_{\Lambda}\text{Be}$  by about 0.9 MeV, part of which must arise from going beyond the  $s$ -wave dominant  $(\ell, \lambda)=(0,0)$  component (98.0% probability weight). This overbinding of  ${}^9_{\Lambda}\text{Be}$  was subsequently cured phenomenologically by Hiyama *et al.* [14] by weakening the  $p$ -wave component of the underlying  $\Lambda N$  interaction; alternatively it can be cured introducing a repulsive  $\Lambda\alpha\alpha$  interaction potential to simulate a likely contribution due to  $\Lambda NN$  three-body forces [7]. Since our interest in  ${}^9_{\Lambda}\text{Be}$  in this work is mostly for using it as a subsystem input to calculating  ${}^10_{\Lambda\Lambda}\text{Be}$ , we should strive to use a model that reproduces as closely as possible the binding energies of such subsystems. The significance of this requirement, in the framework of a Faddeev calculation for  ${}^3_{\Lambda}\text{H}$ , was emphasized in Ref. [36]. Indeed, our  $s$ -wave Faddeev calculation for  ${}^9_{\Lambda}\text{Be}$  nearly reproduces the observed binding energy. The effect of the higher partial waves  $(\ell, \lambda)=(2,2),(4,4)$  ignored by us must be largely cancelled out in the evaluation of  $\Delta B_{\Lambda\Lambda}({}^{10}_{\Lambda\Lambda}\text{Be})$  as defined later on.

Having thus gained confidence in the appropriateness of the  $\alpha\alpha$  and  $\Lambda\alpha$  input potentials, we then applied these potentials to the solution of the Faddeev-Yakubovsky equations for  ${}^6_{\Lambda\Lambda}\text{He}$  and  ${}^{10}_{\Lambda\Lambda}\text{Be}$ , using different  $\Lambda\Lambda$  interactions generically of the form (24).



### A. ${}_{\Lambda\Lambda}{}^6\text{He}$ and ${}_{\Lambda\Lambda}{}^{10}\text{Be}$

The ground-state energies  $E_{\Lambda\Lambda}$  obtained by solving the  $s$ -wave three-body ( $\alpha\Lambda\Lambda$ ) Faddeev equations for  ${}_{\Lambda\Lambda}{}^6\text{He}$  and the  $s$ -wave four-body ( $\alpha\alpha\Lambda\Lambda$ ) Yakubovsky equations for  ${}_{\Lambda\Lambda}{}^{10}\text{Be}$  are given in Table V for  $\Lambda\Lambda$  potentials ordered according to their degree of attraction. The corresponding  $\Lambda\Lambda$  binding energies  $B_{\Lambda\Lambda}$  are given by  $B_{\Lambda\Lambda} = -E_{\Lambda\Lambda}$  for  ${}_{\Lambda\Lambda}{}^6\text{He}$  and  $B_{\Lambda\Lambda} = -(E_{\Lambda\Lambda} + 0.1 \text{ MeV})$  for  ${}_{\Lambda\Lambda}{}^{10}\text{Be}$ . The strongest  $\Lambda\Lambda$  attraction is provided by the potential of the uppermost row, simulating the very recent ESC00 model [11] which was partly motivated by wishing to get a  $B_{\Lambda\Lambda}$  value for  ${}_{\Lambda\Lambda}{}^6\text{He}$  as close to that reported by Prowse [3]; indeed our calculation reproduces it. Significantly lower  $B_{\Lambda\Lambda}$  values are obtained for our simulation of model ND which, however, reproduces well the  $B_{\Lambda\Lambda}$  value reported for  ${}_{\Lambda\Lambda}{}^{10}\text{Be}$  [17]. These calculated  $B_{\Lambda\Lambda}$  values were obtained using a  $\Lambda\Lambda$  potential of the form (24), very similar to but not identical with the one (also marked ND) used in the cluster calculation [14] which is listed separately in the table. The appropriate low-energy parameters, also shown in Table V, are very close to each other, and the variation thereby induced in the calculated  $B_{\Lambda\Lambda}({}_{\Lambda\Lambda}{}^6\text{He})$  is merely 0.03 MeV within our own  $s$ -wave calculation. Furthermore, our calculation essentially agrees with that of Ref. [14] for  ${}_{\Lambda\Lambda}{}^6\text{He}$ , whereas for  ${}_{\Lambda\Lambda}{}^{10}\text{Be}$  our calculation provides about 0.5 MeV more binding. In view of the restriction of our calculation to  $s$  waves, its rough agreement with that of Ref. [14] for  ${}_{\Lambda\Lambda}{}^{10}\text{Be}$  should be considered satisfactory. We note that the variation within the various calculations of Ref. [14] for  $B_{\Lambda\Lambda}({}_{\Lambda\Lambda}{}^{10}\text{Be})$ , as function of the microscopically-motivated  $\Lambda\alpha$  interactions used by these authors, exceeds 0.5 MeV. We feel that typical errors due to limiting our calculations to  $s$  waves are a fraction of 0.5 MeV for  ${}_{\Lambda\Lambda}{}^6\text{He}$  (as discussed in Sect. IV) and about 0.5 MeV for  ${}_{\Lambda\Lambda}{}^{10}\text{Be}$ . In addition to the simulation of the *bare*  $\Lambda\Lambda$  ND interaction discussed above, we also listed in Table V binding energies calculated for a simulation of the  $G$ -matrix constructed in Ref. [37] out of the ND bare interaction. This was done for the sole purpose of comparing below our calculation to those of Refs. [16,37]; of course, using a  $G$ -matrix interaction rather than a bare interaction within a full-space calculation is fraught with double counting and should be avoided as properly acknowledged in the subsequent work of Ref. [14]. Down the list in Table V, the NSC97 models are seen to give yet lower  $B_{\Lambda\Lambda}$  values, which for  ${}_{\Lambda\Lambda}{}^6\text{He}$  are close to the very recent experimental report [9]. In between the rows pertaining to model ND and those for model NSC97, just for interpolation, we also listed results for two intermediate-strength  $\Lambda\Lambda$  interaction potentials specified by their low-energy parameters.

In Tables VI and VII we list information on the geometrical sizes of  ${}_{\Lambda\Lambda}{}^6\text{He}$  and  ${}_{\Lambda\Lambda}{}^{10}\text{Be}$ , respectively. As expected, the stronger the  $\Lambda\Lambda$  interaction is – the smaller are the geometrical sizes of these few-body systems. We note, without offering any explanation for it, that almost all of our calculated sizes, particularly for  ${}_{\Lambda\Lambda}{}^{10}\text{Be}$ , are significantly larger than those calculated in Ref. [14] which is the only comprehensive calculation accounting for all rearrangement channels to compare with. An interesting exception is provided by the r.m.s. distance between the two  $\alpha$  clusters in  ${}_{\Lambda\Lambda}{}^{10}\text{Be}$ :  $R_{\alpha\alpha} = 3.4 \text{ fm}$  in both calculations for model ND, in spite of the radically different  $\alpha\alpha$  potentials used in these calculations. With such a large value of  $R_{\alpha\alpha}$ , the two  $\alpha$  clusters apparently are little affected by the inner part of their potential, which for a more compressed configuration would require a better theoretical guidance than provided by the Ali-Bodmer potential [29] used by us. This insensitivity to the inner structure of the  $\alpha$  clusters, when  $\Lambda$ 's are added, no longer holds when nucleons are

added; for example, for the  $3\alpha$  system, where  $R_{\alpha\alpha} = 3.0$  fm in typical  $^{12}\text{C}$   $0^+$  ground-state calculations. Thus, Fedorov and Jensen [38], using the Ali-Bodmer  $\alpha\alpha$  potential, had to introduce a strongly *attractive*  $3\alpha$  potential in order to nearly reproduce the energies of the two lowest  $0^+$  states in  $^{12}\text{C}$ , whereas Hiyama *et al.* [14], excluding Pauli-forbidden  $\alpha\alpha$  states from their  $\alpha\alpha$  potential, had to introduce a strongly *repulsive*  $3\alpha$  potential.

For  ${}_{\Lambda\Lambda}^6\text{He}$  we also listed in Table VI the probability (4) of having it as a two-body  $(\alpha\Lambda)-\Lambda$  cluster. This probability goes to one as  $V_{\Lambda\Lambda}$  approaches zero; the structure of  ${}_{\Lambda\Lambda}^6\text{He}$  is then well approximated by a  ${}^5_{\Lambda}\text{He} - \Lambda$  cluster, and the r.m.s. distance  $R_{\Lambda\alpha}$  between one of the  $\Lambda$  hyperons and the  $\alpha$  cluster is only slightly smaller than the value  $R_{\Lambda\alpha}({}^5_{\Lambda}\text{He}) = 3.16$  fm. On the other hand, the value of the analogous r.m.s. distance between one of the  $\Lambda$  hyperons and the c.m. of the  $\alpha\alpha$  clusters in  ${}^{10}_{\Lambda\Lambda}\text{Be}$ ,  $R_{(\alpha\alpha)\Lambda} = 3.26$  fm as shown in Table VII for  $V_{\Lambda\Lambda} \rightarrow 0$ , is considerably larger than the value  $R_{(\alpha\alpha)\Lambda}({}^9_{\Lambda}\text{Be}) = 2.88$  fm, indicating that the two-body clustering  ${}^9_{\Lambda}\text{Be} - \Lambda$  is far from saturating the structure of  ${}^{10}_{\Lambda\Lambda}\text{Be}$  in this limit. This point, as well as the information given in parentheses in Table VII, will be discussed in more detail towards the end of the subsection. A final point in discussing Tables VI and VII concerns the ground-state energies  $E_{\Lambda\Lambda}$  calculated for the  $G$ -matrix interaction ND(G) based on the bare ND interaction. Our calculated binding energy for  ${}_{\Lambda\Lambda}^6\text{He}$  is higher by about 0.8 MeV than that calculated in Refs. [16,37]. Given the fact that our calculation for the ND interaction comes very close within that of the complete calculation of Hiyama *et al.* [14], we conclude that the calculations of Refs. [16,37] are far from being complete.

It has been shown in previous cluster calculations [7,8] that the calculated  $B_{\Lambda\Lambda}$  values for  ${}_{\Lambda\Lambda}^6\text{He}$  and for  ${}_{\Lambda\Lambda}^{10}\text{Be}$  are correlated nearly linearly with each other. Our calculations also indicate such a correlation, as demonstrated in Fig. 3 by the dotted line. This line precludes any joint theoretical explanation of the  ${}_{\Lambda\Lambda}^6\text{He}$  and  ${}_{\Lambda\Lambda}^{10}\text{Be}$  experimental candidates listed in Table V. If  $B_{\Lambda\Lambda}({}^{10}_{\Lambda\Lambda}\text{Be}) = 17.7 \pm 0.4$  MeV [2,17], then the theoretically implied  $B_{\Lambda\Lambda}$  value for  ${}_{\Lambda\Lambda}^6\text{He}$  is about  $9.1 \pm 0.4$  MeV, considerably below the value reported by Prowse [3] but considerably above the value reported very recently by Takahashi *et al.* [9]. If  $B_{\Lambda\Lambda}({}^{10}_{\Lambda\Lambda}\text{Be}) = 14.6 \pm 0.4$  MeV, on the assumption that the  $\pi^-$  weak decay of  ${}^{10}_{\Lambda\Lambda}\text{Be}$  ground state occurred to the first excited doublet levels of  ${}^9_{\Lambda}\text{Be}$  at 3.1 MeV [39], then the theoretically implied  $B_{\Lambda\Lambda}$  value for  ${}_{\Lambda\Lambda}^6\text{He}$  is  $6.1 \pm 0.4$  MeV, no longer in such a spectacular disagreement with experiment but still significantly below the value reported by the recent observation [9] of  ${}_{\Lambda\Lambda}^6\text{He}$ .

For  $V_{\Lambda\Lambda} = 0$ , the lower-left point on the dotted line marked ‘4-body model’ in Fig. 3 corresponds to approximately zero incremental binding energy  $\Delta B_{\Lambda\Lambda}$  for  ${}_{\Lambda\Lambda}^6\text{He}$ , where

$$\Delta B_{\Lambda\Lambda}({}_{\Lambda\Lambda}^AZ) = B_{\Lambda\Lambda}({}_{\Lambda\Lambda}^AZ) - 2B_{\Lambda}({}_{\Lambda}^{A-1}Z) . \quad (26)$$

This is also explicitly listed in Table VIII and is anticipated owing to the rigidity of the  $\alpha$  core. However, the corresponding  $\Delta B_{\Lambda\Lambda}$  value for  ${}_{\Lambda\Lambda}^{10}\text{Be}$  is fairly substantial, about 1.5 MeV, reflecting a basic difference between the four-body  $\alpha\alpha\Lambda\Lambda$  calculation and any three-body approximation in terms of a nuclear core and two  $\Lambda$ ’s as in  ${}_{\Lambda\Lambda}^6\text{He}$ . To demonstrate this point we show by the dot-dash line marked ‘3-body model’ in Fig. 3 the results of a three-body calculation for  ${}_{\Lambda\Lambda}^{10}\text{Be}$  in which the  ${}^8\text{Be}$  core is not assigned an  $\alpha\alpha$  structure. In this calculation, the  $\Lambda-{}^8\text{Be}$  potential was chosen in a Woods-Saxon form, with depth  $V_0 = 18.12$  MeV, radius  $R = 3.24$  fm and diffusivity  $a = 0.60$  fm. The geometry and depth were fixed by requiring (i) that the ground-state binding energy of the  $\Lambda-{}^8\text{Be}$  system agrees

with that calculated in the  $\alpha\alpha\Lambda$  model calculation for  $B_\Lambda(^9_\Lambda\text{Be})$  (see Table IV); and (ii) that the  $\Lambda$ - $^8\text{Be}$  r.m.s. distance in the  $^9_\Lambda\text{Be}$  ground state agrees with that between the  $\Lambda$  and the c.m. of the two  $\alpha$ 's in the  $\alpha\alpha\Lambda$  model calculation for  $^9_\Lambda\text{Be}$  (2.85 fm *vs.* 2.88 fm, respectively). This three-body calculation for  $^{10}_{\Lambda\Lambda}\text{Be}$ , as is evident from the values given in parentheses in Table VII, gives smaller  $B_{\Lambda\Lambda}$  values by about 1.7 MeV and also smaller geometrical sizes than those given by the four-body calculation. The difference is due to the  $\alpha\alpha$  correlations which are absent in the three-body calculation, and which are built in within the Yakubovsky equations of the four-body calculation. By breaking up  $^8\text{Be}$  into two  $\alpha$ 's in the four-body calculation, substantial attraction is gained due to several additional bound subsystems such as for the  $^6_{\Lambda\Lambda}\text{He} - \alpha$  and the  $^5_\Lambda\text{He} - ^5_\Lambda\text{He}$  clusters which almost saturate the corresponding rearrangement channels  $(\alpha\Lambda\Lambda) - \alpha$  and  $(\alpha\Lambda) - (\alpha\Lambda)$ , respectively. The prominence of these channels is exhibited in Table IX where the probability weights of the various rearrangement-channel components of the  $^{10}_{\Lambda\Lambda}\text{Be}$  ground-state wavefunction are listed, using the generic expression (4). It is striking how little the  $(\alpha\alpha) - (\Lambda\Lambda)$  rearrangement channel contributes to the four-body calculation. Other calculations [7,8] which pointed out the linear relationship discussed above did not account for the full range of 'attractive' rearrangement channels and consequently found smaller values, not exceeding 0.5 MeV, for the  $\Delta B_{\Lambda\Lambda}(^{10}_{\Lambda\Lambda}\text{Be})$  gain as  $V_{\Lambda\Lambda} \rightarrow 0$ .

### B. The $A = 5$ $\Lambda\Lambda$ hypernuclei

The  $A = 5$  isodoublet hypernuclei  $^5_{\Lambda\Lambda}\text{H}$  and  $^5_{\Lambda\Lambda}\text{He}$  were considered by us as three-cluster systems  $^3\text{H} \Lambda\Lambda$  and  $^3\text{He} \Lambda\Lambda$ , respectively. The results of Faddeev calculations for these species were included in Table VIII, in terms of the incremental binding energy  $\Delta B_{\Lambda\Lambda}$  (26), together with results for  $^6_{\Lambda\Lambda}\text{He}$  and  $^{10}_{\Lambda\Lambda}\text{Be}$ . We note that  $\Delta B_{\Lambda\Lambda}$  for  $^5_{\Lambda\Lambda}\text{He}$  is slightly larger than for  $^5_{\Lambda\Lambda}\text{H}$ , owing to the tighter binding of the core  $\Lambda$  hypernucleus  $^4_\Lambda\text{He}$  as compared to  $^4_\Lambda\text{H}$ . The  $A = 5$   $\Lambda\Lambda$  hypernuclei are found to be particle stable for all the  $\Lambda\Lambda$  attractive potentials used in the present calculation. As the  $\Lambda\Lambda$  interaction strength goes to zero,  $\Delta B_{\Lambda\Lambda}(A = 5)$  approaches approximately zero, similarly to  $\Delta B_{\Lambda\Lambda}(A = 6)$ , provided  $\Delta B_{\Lambda\Lambda}(A=5)$  is defined *with respect to the  $(2J+1)$  average* of the  $(^4_\Lambda\text{H}, ^4_\Lambda\text{He})$  levels of Table IV (this is a physically meaningful definition of  $\Delta B_{\Lambda\Lambda}$  when several spin-flip nuclear core levels contribute to the Faddeev calculation; see also the comment made following Eq. (7) for the wavefunction of these  $A = 5$   $\Lambda\Lambda$  hypernuclei). We recall that both of the  $A = 5, 6$   $\Lambda\Lambda$  hypernuclear systems are treated here as three-body clusters. A nearly linear correlation appears between  $\Delta B_{\Lambda\Lambda}(A = 6)$  and  $\Delta B_{\Lambda\Lambda}(A = 5)$ , as shown in Fig. 4. Judging by the slope of the straight lines prevailing over most of the interval shown in the figure, the  $\Lambda\Lambda$  interaction is more effective in binding  $^6_{\Lambda\Lambda}\text{He}$  than binding either one of the  $A = 5$   $\Lambda\Lambda$  hypernuclei. For this range of mass values, the heavier the nuclear core is – the larger  $\Delta B_{\Lambda\Lambda}$  is (except for a vanishingly weak  $V_{\Lambda\Lambda}$  where the trend is opposite), implying that no saturation is yet reached. Within such three-body models  $\Delta B_{\Lambda\Lambda}$  appears to get saturated already about  $A = 10$ , judging by the slope of the three-body calculation straight line of Fig. 3. However, the special four-body cluster structure of  $^{10}_{\Lambda\Lambda}\text{Be}$  reverses this trend of saturation, apparently delaying it into somewhat heavier species (for considerably heavier nuclear cores  $\Delta B_{\Lambda\Lambda}$  should start occasionally decreasing slowly to zero with  $A$ ).

We have already compared our calculations, discussing Tables V,VI,VII, with those of

Ref. [14]. In Table VIII we also added a comparison with the calculations of Ref. [15]. Their  $\Delta B_{\Lambda\Lambda}$  values are incredibly higher everywhere than ours, and this holds also for their ND-type calculation of  ${}^5_{\Lambda}\text{He}$ .

#### IV. SUMMARY

In this work we studied light  $\Lambda\Lambda$  hypernuclear systems which may be described in terms of few-cluster systems and treated by solving the three-body Faddeev and four-body Faddeev-Yakubovsky  $s$ -wave differential equations. For  ${}^{10}_{\Lambda\Lambda}\text{Be}$ , the Faddeev-Yakubovsky solution of the  $\alpha\alpha\Lambda\Lambda$  problem given here is the first one of its kind. We estimate an error of about 0.5 MeV due to limiting the  ${}^{10}_{\Lambda\Lambda}\text{Be}$  calculation to  $s$  waves. Our calculation yields more binding for  ${}^{10}_{\Lambda\Lambda}\text{Be}$  than that produced by most of the previous calculations, wherever comparison is meaningful. In particular, a fairly large value of  $\Delta B_{\Lambda\Lambda} \sim 1.5$  MeV survives in the limit  $V_{\Lambda\Lambda} \rightarrow 0$  owing to the  $\alpha\alpha$  structure of the  ${}^8\text{Be}$  core. Our calculation confirms, if not aggravates, the incompatibility of the ‘old’ experimental determination of the binding energy of  ${}^6_{\Lambda\Lambda}\text{He}$  [3] with that of  ${}^{10}_{\Lambda\Lambda}\text{Be}$  [2] in accordance with previous cluster calculations, irrespective of whether or not three-body  $\Lambda\alpha\alpha$  interactions are included (see e.g. Refs. [7,14] respectively). The ‘new’ experimental determination of the binding energy of  ${}^6_{\Lambda\Lambda}\text{He}$  [9] is found to be even more incompatible with that of  ${}^{10}_{\Lambda\Lambda}\text{Be}$ . Assuming that the determination of  $B_{\Lambda\Lambda}({}^{10}_{\Lambda\Lambda}\text{Be})$  was plagued by an unobserved  $\gamma$  deexcitation involving either  ${}^{10}_{\Lambda\Lambda}\text{Be}^*$  or  ${}^9_{\Lambda}\text{Be}^*$ , somewhere along the sequence of tracks observed in the emulsion event carefully reanalyzed in Ref. [17], does not satisfactorily resolve this incompatibility. Adding  ${}^{13}_{\Lambda\Lambda}\text{B}$  [4] as input does not alleviate it either, since the possibility of unobserved  $\gamma$  deexcitation cannot be dismissed also for this species, while on the theoretical side the analysis of  ${}^{13}_{\Lambda\Lambda}\text{B}$  in terms of a few-cluster system is more dubious than for the lighter  $\Lambda\Lambda$  species. Our conclusion differs radically from the recent claim of compatibility by Albertus *et al.* [40] who used a different methodology, largely untested in studies of very light nuclear species.

Discarding the past history of emulsion experimentation for  $\Lambda\Lambda$  hypernuclear events identified as heavier than  ${}^6_{\Lambda\Lambda}\text{He}$ , because of the ambiguities mentioned here, one remains with the very recent report from the KEK E373 experiment [9] which claims to have identified uniquely  ${}^6_{\Lambda\Lambda}\text{He}$ , with  $\Delta B_{\Lambda\Lambda} \sim 1$  MeV. No particle-stable excited states are possible for this species or for its  $\Lambda$  hypernuclear core  ${}^5_{\Lambda}\text{He}$ , so this event - if confirmed by adding more events of its kind - should be taken as the most directly relevant constraint on the  $\Lambda\Lambda$  interaction. Moreover,  ${}^6_{\Lambda\Lambda}\text{He}$  is ideally suited for three-body cluster calculations such as the Faddeev equations here solved for the  $\alpha\Lambda\Lambda$  system. Using  $s$ -wave soft-core  $\Lambda\Lambda$  potentials that simulate several of the Nijmegen  $\Lambda\Lambda$  interaction models, we have shown that such simulations of model NSC97, versions  $e$  and  $f$  of which have been shown recently to agree quantitatively with data on light  $\Lambda$  hypernuclei [18,41], are capable of nearly reproducing the new value [9] of  $\Delta B_{\Lambda\Lambda}({}^6_{\Lambda\Lambda}\text{He})$ , short by about 0.5 MeV of the mean value.\* In fact, we

---

\*in order to precisely reproduce this mean value, the parameter  $\gamma$  needs to be increased from its values listed in Table II for model NSC97 to 0.6598, yielding the following low-energy parameters:  $a_{\Lambda\Lambda} = -0.77$  fm,  $r_{\Lambda\Lambda} = 6.59$  fm.

estimate the theoretical uncertainty of our Faddeev calculation for  ${}_{\Lambda\Lambda}{}^6\text{He}$  as a fraction of 0.5 MeV. Two approximations give rise to this theoretical uncertainty, one is the restriction to  $s$ -waves in the partial-wave expansion of the Faddeev equations, excluding higher  $\ell$  values; the other one is ignoring the off-diagonal  $\Lambda\Lambda - \Xi N$  interaction which admixes  $\Xi$  components into the  ${}_{\Lambda\Lambda}{}^6\text{He}$  wavefunction. The following estimates may be given for the errors incurred in these approximations. As for the  $s$ -wave approximation, the calculations by Ikeda *et al.* [42] give 99.7% probability weight for the  $(\ell, \lambda)=(0,0)$  channel, with higher partial waves adding only 0.3 MeV binding energy, well within the error bars of the measured energies. As for including explicitly the  $\Lambda\Lambda - \Xi N$  coupling, a recent work by Yamada and Nakamoto [16] using model ND(G) (another model) finds an increase of 0.4 (0.1) MeV in the calculated  $B_{\Lambda\Lambda}({}_{\Lambda\Lambda}{}^6\text{He})$  value due to including explicitly the  $\Lambda\Lambda - \Xi N$  coupling, resulting in a 0.3% (0.1%) probability  $\Xi$  component. Carr *et al.* [43] found a similar increase of 0.2 MeV due to explicitly including this coupling, for a  $\Lambda\Lambda$  interaction comparable to those used in the present work. However, these authors pointed out that, with respect to a calculation using an *effective* single-channel  $\Lambda\Lambda$  interaction which implicitly includes the effect of  $\Lambda\Lambda - \Xi N$  coupling in free space, an explicit two-channel calculation for  ${}_{\Lambda\Lambda}{}^6\text{He}$  yields a reduction of  $B_{\Lambda\Lambda}({}_{\Lambda\Lambda}{}^6\text{He})$  by about 0.3 MeV. This reduction is expected due to the tight binding of the  $\alpha$  cluster which inhibits the effectiveness of the  $\Lambda\Lambda - \Xi N$  coupling. Therefore, the effects of the two approximations here discussed tend to cancel each other almost completely. This conclusion should also hold qualitatively for  ${}_{\Lambda\Lambda}{}^{10}\text{Be}$  due to the fairly large energy which the  $\Lambda\Lambda - \Xi N$  coupling requires in order to break an  $\alpha$  constituent.

If model NSC97, as our few-body calculations suggest, provides for the right SU(3) extrapolation from fits to  $NN$  and  $YN$  data, then it is questionable whether  ${}_{\Lambda\Lambda}{}^4\text{H}$  is particle stable. The subtleties involved in estimating whether or not this species provides for the onset of  $\Lambda\Lambda$  binding in nuclei were clearly demonstrated in Ref. [44]. Its  $\Delta B_{\Lambda\Lambda}$ , at any rate, should not exceed 0.5 MeV for considerably stronger  $\Lambda\Lambda$  interactions [15]. If the AGS E906 events conjectured in Ref. [10] as evidence for  ${}_{\Lambda\Lambda}{}^4\text{H}$  are confirmed as such in a future extension of this experiment, this four-body system  $pn\Lambda\Lambda$  would play as a fundamental role for studying theoretically the hyperon-hyperon forces as  ${}^3_{\Lambda}\text{H}$  ( $pn\Lambda$ ) has played for studying theoretically the hyperon-nucleon forces [45]. Our preliminary results, studying the solutions of the Faddeev-Yakubovsky equations for the  $pn\Lambda\Lambda$  system, indicate that  ${}_{\Lambda\Lambda}{}^4\text{H}$  is unstable against  $\Lambda$  emission.

A.G. would like to acknowledge useful discussions and correspondence with Toshio Motoba. This work was partially supported by the Israel Science Foundation (grant 131/01). I.N.F. is also partly supported by the Russian Ministry of Education (grant E00-3.1-133).

## REFERENCES

- [1] J. Schaffner-Bielich and A. Gal, Phys. Rev. C **62**, 034311 (2000).
- [2] M. Danysz *et al.*, Nucl. Phys. **49**, 121 (1963).
- [3] D.J. Prowse, Phys. Rev. Lett. **17**, 782 (1966).
- [4] S. Aoki *et al.*, Prog. Theor. Phys. **85**, 1287 (1991).
- [5] C.B. Dover, D.J. Millener, A. Gal and D.H. Davis, Phys. Rev. C **44**, 1905 (1991).
- [6] Y. Yamamoto, H. Takaki and K. Ikeda, Prog. Theor. Phys. **86**, 867 (1991).
- [7] A.R. Bodmer, Q.N. Usmani and J. Carlson, Nucl. Phys. A **422**, 510 (1984).
- [8] X.C. Wang, H. Takaki and H. Bando, Prog. Theor. Phys. **76**, 865 (1986).
- [9] H. Takahashi *et al.*, Phys. Rev. Lett. **87**, 212502 (2001).
- [10] J.K. Ahn *et al.*, Phys. Rev. Lett. **87**, 132504 (2001).
- [11] Th.A. Rijken, Nucl. Phys. A **691**, 322c (2001).
- [12] A. Reuber, K. Holinde and J. Speth, Nucl. Phys. A **570**, 543 (1994).
- [13] Y. Fujiwara, C. Nakamoto and Y. Suzuki, Phys. Rev. C **54**, 2180 (1996).
- [14] E. Hiyama, M. Kamimura, T. Motoba, T. Yamada and Y. Yamamoto, Prog. Theor. Phys. **97**, 881 (1997).
- [15] H. Nemura, Y. Suzuki, Y. Fujiwara and C. Nakamoto, Prog. Theor. Phys. **103**, 929 (2000).
- [16] T. Yamada and C. Nakamoto, Phys. Rev. C **62**, 034319 (2000).
- [17] R.H. Dalitz, D.H. Davis, P.H. Fowler, A. Montwill, J. Pniewski and J.A. Zakrzewski, Proc. Roy. Soc. London A **426**, 1 (1989).
- [18] Th.A. Rijken, V.G.J. Stoks and Y. Yamamoto, Phys. Rev. C **59**, 21 (1999).
- [19] V.G.J. Stoks and Th.A. Rijken, Phys. Rev. C **59**, 3009 (1999).
- [20] I.N. Filikhin and A. Gal, Phys. Rev. C **65**, 041001(R) (2002).
- [21] L.D. Faddeev and S.P. Merkuriev, *Quantum Scattering Theory for Several Particle Systems* (Kluwer Academic, Dordrecht, 1993).
- [22] I.N. Filikhin and S.L. Yakovlev, Phys. At. Nucl. **63**, 336 (2000).
- [23] S.P. Merkuriev, S.L. Yakovlev and C. Gignoux, Nucl. Phys. A **431**, 125 (1984).
- [24] H. Kamada and W. Gloeckle, Nucl. Phys. A **548**, 205 (1992).
- [25] S.L. Yakovlev and I.N. Filikhin, Phys. At. Nucl. **58**, 754 (1995); *ibid.* **60**, 1794 (1997).
- [26] I.N. Filikhin and S.L. Yakovlev, Phys. At. Nucl. **62**, 1490 (1999); *ibid.* **63**, 55 (2000); *ibid.* **63**, 69 (2000).
- [27] I.N. Filikhin and S.L. Yakovlev, Phys. At. Nucl. **63**, 223 (2000).
- [28] M.M. Nagels, T.A. Rijken and J.J. de Swart, Phys. Rev. D **12**, 744 (1975); *ibid.* **15**, 2547 (1977).
- [29] S. Ali and A.R. Bodmer, Nucl. Phys. **80**, 99 (1966).
- [30] I. Kumagai-Fuse, S. Okabe, and Y. Akaishi, Phys. Lett. B **345**, 386 (1995).
- [31] H. Nemura, Y. Akaishi and Y. Suzuki, nucl-th/0203013.
- [32] D.H. Davis and J. Pniewski, Contemp. Phys. **27**, 91 (1986); see also D.H. Davis, in *LAMPF Workshop on ( $\pi, K$ ) Physics*, edited by B.F. Gibson, W.R. Gibbs and M.B. Johnson, AIP Conference Proceedings 224, New York, 1991, pp. 38-48.
- [33] M. Bedjidian *et al.*, Phys. Lett. B **83**, 252 (1979).
- [34] H. Bando, K. Ikeda and T. Motoba, Prog. Theor. Phys. **67**, 508 (1982).
- [35] T. Motoba, H. Bando, K. Ikeda and T. Yamada, Prog. Theor. Phys. Suppl. **81**, 42 (1985).

- [36] A. Cobis, A.S. Jensen and D.V. Fedorov, J. Phys. G **23**, 401 (1997).
- [37] Y. Yamamoto, T. Motoba, H. Himeno, K. Ikeda and S. Nagata, Prog. Theor. Phys. Suppl. **117**, 361 (1994).
- [38] D.V Fedorov and A.S. Jensen, Phys. Lett. B **389**, 631 (1996).
- [39] M. May *et al.*, Phys. Rev. Lett. **51**, 2085 (1983).
- [40] C. Albertus, J.E. Amaro and J. Nieves, nucl-th/0110046.
- [41] Y. Akaishi, T. Harada, S. Shinmura, and Khin Swe Myint, Phys. Rev. Lett. **84**, 3539 (2000); H. Nemura, Y. Akaishi and Y. Suzuki, nucl-th/0203013.
- [42] K. Ikeda, H. Bando and T. Motoba, Prog. Theor. Phys. Suppl. **81**, 147 (1985).
- [43] S.B. Carr, I.R. Afnan and B.F. Gibson, Nucl. Phys. A **625**, 143 (1997).
- [44] S. Nakaichi-Maeda and Y. Akaishi, Prog. Theor. Phys. **84**, 1025 (1990).
- [45] K. Miyagawa, H. Kamada, W. Gloeckle and V. Stoks, Phys. Rev. C **51**, 2905 (1995); K. Miyagawa, H. Kamada, W. Gloeckle, H. Yamamoto, T. Mart and C. Bennhold, Few-Body Syst. Suppl. **12**, 324 (2000).

TABLES

TABLE I. Parameters of the potential (24) simulating  $\Lambda\Lambda$   $^1S_0$  Nijmegen interaction potentials.

$i$	$\beta_i$ (fm)	$v^{(i)}$ (MeV)
1	1.342	-21.49
2	0.777	-379.1 $\gamma$
3	0.350	9324

TABLE II.  $\Lambda\Lambda$   $^1S_0$  scattering lengths  $a$  and effective ranges  $r$  for several Nijmegen potential models. The values in parentheses correspond to using the form (24), with parameters from Table I plus the values of  $\gamma$  listed here to simulate these potentials.

Parameter	NSC97b	NSC97e	NSC97f	ND	ESC00
$a_{\Lambda\Lambda}$ (fm)	-0.38 (-0.38)	-0.50 (-0.50)	-0.35 (-0.36)	-2.80 (-2.81)	-10.6 (-10.6)
$r_{\Lambda\Lambda}$ (fm)	10.24 (15.2)	9.11 (10.6)	14.68 (16.6)	2.81 (2.95)	2.7 (2.23)
$\gamma$	0.4804	0.5463	0.4672	1	1.2044

TABLE III. Parameters of the Isle potential (25) for the  $\alpha\alpha$  and  $\Lambda\alpha$  interactions.

$j$	$V_{\text{rep}}^{(j)}$ (MeV)	$\beta_{\text{rep}}^{(j)}$ (fm)	$V_{\text{att}}^{(j)}$ (MeV)	$\beta_{\text{att}}^{(j)}$ (fm)
$\alpha\alpha$ [29]	120.0	1.53	30.18	2.85
$\Lambda\alpha$ [30]	450.4	1.25	404.9	1.41

TABLE IV. Binding energies  $B_\Lambda$  of  $\Lambda$  hypernuclei.

	$^4_\Lambda\text{H}(0^+)$	$^4_\Lambda\text{H}(1^+)$	$^4_\Lambda\text{He}(0^+)$	$^4_\Lambda\text{He}(1^+)$	$^5_\Lambda\text{He}$	$^9_\Lambda\text{Be}$
$\beta_{\text{rep}}$ (fm)	1.2573	1.2720	1.2532	1.2687	1.25	-
$B_\Lambda^{\text{calc.}}$ (MeV)	2.06	1.04	2.36	1.24	3.09	6.64
$B_\Lambda^{\text{exp.}}$ (MeV)	$2.04 \pm 0.04^a$	$1.00 \pm 0.04^b$	$2.39 \pm 0.03^a$	$1.24 \pm 0.04^b$	$3.12 \pm 0.02^a$	$6.71 \pm 0.04^a$

<sup>a</sup>Ref. [32]    <sup>b</sup>Ref. [33]



TABLE V. Calculated ground-state energies of  $\Lambda\Lambda$  hypernuclei  $E_{\Lambda\Lambda}$  (in MeV) with respect to the breakup threshold of the free clusters, using  $\alpha\alpha$  and  $\Lambda\alpha$  potentials of the form (25) with parameters listed in Table III, for  $\Lambda\Lambda$  potentials (24) simulated by fitting to the scattering length  $a$  and effective range  $r$  (in fm) of several Nijmegen interaction models.

Model	${}^5_{\Lambda}\text{He}$	${}^9_{\Lambda}\text{Be}$	$a_{\Lambda\Lambda}$	$r_{\Lambda\Lambda}$	${}^6_{\Lambda\Lambda}\text{He}$	${}^{10}_{\Lambda\Lambda}\text{Be}$
ESC00	-3.09	-6.55	-10.6	2.23	-10.7	-19.4
ND(G) <sup>a</sup>			-5.37	2.40	-10.1	-18.7
ND			-2.81	2.95	-9.10	-17.7
–			-0.77	2.92	-7.70	-16.4
–			-0.31	3.12	-6.98	-15.6
NSC97e			-0.50	10.6	-6.82	-15.4
NSC97b			-0.38	15.2	-6.60	-15.2
$V_{\Lambda\Lambda} = 0$			0.0	–	-6.27	-14.8
[14] ND	-3.12	-6.67	-2.80	2.81	-9.34	-17.15
exp.	$-3.12 \pm 0.02^b$	$-6.62 \pm 0.04^b$	–	–	$-10.9 \pm 0.6^c$ $-7.25 \pm 0.19^{+0.18}_{-0.11}{}^e$	$-17.6 \pm 0.4^d$ $-14.5 \pm 0.4^f$

<sup>a</sup>Ref. [37] <sup>b</sup>Ref. [32] <sup>c</sup>Ref. [3] <sup>d</sup>Ref. [17] <sup>e</sup>Ref. [9] <sup>f</sup>assuming  ${}^{10}_{\Lambda\Lambda}\text{Be} \rightarrow \pi^- + p + {}^9_{\Lambda}\text{Be}^*$

TABLE VI. Ground-state energies  $E_{\Lambda\Lambda}$  of  ${}^6_{\Lambda\Lambda}\text{He}$  calculated for an  $\alpha\Lambda\Lambda$  system; the r.m.s distance between the  $\Lambda$  hyperons ( $R_{\Lambda\Lambda}$ ), between the center of mass of the hyperon pair to the  $\alpha$  cluster ( $R_{(\Lambda\Lambda)\alpha}$ ) and between one of the  $\Lambda$  hyperons to the  $\alpha$  cluster ( $R_{\Lambda\alpha}$ ); the probability weight ( $P_{(\Lambda\alpha)-\Lambda}$ ) using Eq. (4) for the rearrangement channel  $(\Lambda\alpha) - \Lambda$ , for various  $\Lambda\Lambda$  interaction models.

Model	$E_{\Lambda\Lambda}$ (MeV)	$R_{\Lambda\Lambda}$ (fm)	$R_{(\Lambda\Lambda)\alpha}$ (fm)	$R_{\Lambda\alpha}$ (fm)	$P_{(\Lambda\alpha)-\Lambda}$
ESC00	-10.7	3.09	2.04	2.56	0.804
ND(G)	-10.1	3.18	2.06	2.61	0.830
ND	-9.10	3.36	2.11	2.70	0.870
NSC97e	-6.82	3.93	2.29	3.02	0.969
$V_{\Lambda\Lambda} = 0$	-6.27	4.09	2.35	3.12	0.999
[37] ND(G)	-9.23	3.31	2.14		
[16] ND(G)	-9.4				
[14] ND	-9.34	3.20		2.55	

TABLE VII. Ground-state energies  $E_{\Lambda\Lambda}$  of  ${}_{\Lambda\Lambda}^{10}\text{Be}$  calculated for an  $\alpha\alpha\Lambda$  system; the r.m.s distance between the  $\alpha$  clusters ( $R_{\alpha\alpha}$ ), between the  $\Lambda$  hyperons ( $R_{\Lambda\Lambda}$ ), between one of the  $\Lambda$  hyperons and the c.m. of the  $\alpha\alpha$  clusters ( $R_{(\alpha\alpha)\Lambda}$ ) and between the c.m. of the  $\alpha\alpha$  clusters and the c.m. of the  $\Lambda$  hyperons ( $R_{(\alpha\alpha)(\Lambda\Lambda)}$ ), using various  $\Lambda\Lambda$  interaction models. Results for a three-body  ${}^8\text{Be}$   $\Lambda\Lambda$  model are given in parentheses.

Model	$E_{\Lambda\Lambda}$ (MeV)	$R_{\alpha\alpha}$ (fm)	$R_{\Lambda\Lambda}$ (fm)	$R_{(\alpha\alpha)\Lambda}$ (fm)	$R_{(\alpha\alpha)(\Lambda\Lambda)}$ (fm)
ESC00	-19.4 (-17.5)	3.3 –	3.7 (3.2)	2.87 (2.49)	2.2 (1.9)
ND(G)	-18.7 (-17.0)	3.3 –	3.8 (3.3)	2.91 (2.52)	2.3 (1.9)
ND	-17.7 (-16.0)	3.4 –	3.9 (3.4)	3.02 (2.60)	2.3 (2.0)
NSC97e	-15.4 (-13.8)	3.5 –	4.2 (3.7)	3.17 (2.80)	2.4 (2.1)
$V_{\Lambda\Lambda} = 0$	-14.8 (-13.3)	3.6 –	4.3 (3.8)	3.26 (2.85)	2.4 (2.1)
[14] ND	-17.15	3.40	3.02		1.90
[37] ND(G)	(-17.7)	–	(2.81)		(1.67)
[16] ND(G)	(-17.0)	–	(2.8)		

TABLE VIII. Incremental binding energies  $\Delta B_{\Lambda\Lambda}$  (in MeV) for  $\Lambda\Lambda$  potentials (24) specified by the scattering length  $a$  and effective range  $r$  (in fm).  $\Delta B_{\Lambda\Lambda}(A=5)$  is relative to the  $(2J+1)$  average of the ( ${}^4_{\Lambda}\text{H}$ ,  ${}^4_{\Lambda}\text{He}$ ) levels of Table IV.

Model	$a_{\Lambda\Lambda}$	$r_{\Lambda\Lambda}$	${}_{\Lambda\Lambda}^5\text{H}$	${}_{\Lambda\Lambda}^5\text{He}$	${}_{\Lambda\Lambda}^6\text{He}$	${}_{\Lambda\Lambda}^{10}\text{Be}$
ESC00	-10.6	2.23	3.46	3.68	4.51	6.1
ND	-2.81	2.95	2.11	2.27	2.91	4.4
–	-0.77	2.92	1.02	1.13	1.51	3.1
–	-0.31	3.12	0.53	0.59	0.79	2.3
NSC97e	-0.50	10.6	0.50	0.55	0.63	2.1
NSC97b	-0.38	15.2	0.37	0.40	0.41	1.9
$V_{\Lambda\Lambda} = 0$	0	–	0.11	0.12	0.08	1.5
[14] ND	-2.80	2.81	–	–	3.10	3.74
[15] ND	-2.80	2.81	2.8	2.7	4.3	–
exp.					$4.7 \pm 0.6^a$	$4.3 \pm 0.4^b$
					$1.01 \pm 0.20_{-0.11}^{+0.18}$ <sup>c</sup>	$1.2 \pm 0.4$ <sup>d</sup>

<sup>a</sup>Ref. [3] <sup>b</sup>Ref. [17] <sup>c</sup>Ref. [9] <sup>d</sup>assuming  ${}_{\Lambda\Lambda}^{10}\text{Be} \rightarrow \pi^- + p + {}^9_{\Lambda}\text{Be}^*$

TABLE IX. Probability weights of rearrangement channels for  ${}^{10}_{\Lambda\Lambda}\text{Be}$ , evaluated using a generalization of Eq. (4) within a four-body  $\alpha\alpha\Lambda\Lambda$  calculation. In parentheses, the weights for the bound-system clusters are given:  ${}^6_{\Lambda\Lambda}\text{He}$  for  $\alpha\Lambda\Lambda$ ,  ${}^9_{\Lambda}\text{Be}$  for  $\alpha\alpha\Lambda$  and  ${}^5_{\Lambda}\text{He}$  for  $\alpha\Lambda$ .

Model	$P_{(\alpha\Lambda\Lambda)-\alpha}$	$P_{(\alpha\alpha\Lambda)-\Lambda}$	$P_{(\alpha\Lambda)-(\alpha\Lambda)}$	$P_{(\alpha\alpha)-(\Lambda\Lambda)}$
ESC00	0.450 (0.448)	0.314 (0.312)	0.227 (0.224)	0.0095
ND	0.379 (0.378)	0.359 (0.357)	0.253 (0.250)	0.0083
NSC97e	0.276 (0.276)	0.428 (0.424)	0.291 (0.287)	0.0048
$V_{\Lambda\Lambda} = 0$	0.260 (0.247)	0.445 (0.442)	0.290 (0.286)	0.0046

FIGURES

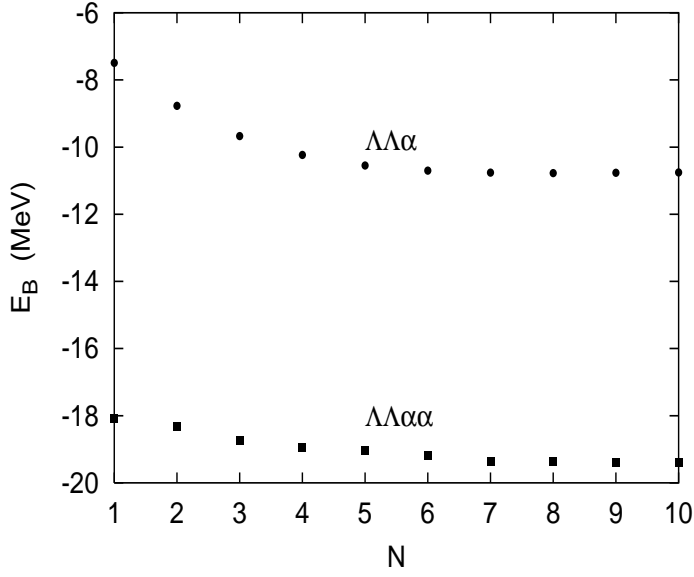


FIG. 1.  ${}_{\Lambda\Lambda}^6\text{He}$  and  ${}_{\Lambda\Lambda}^{10}\text{Be}$  ground-state energies  $E_B$  calculated by solving the  $s$ -wave Faddeev equations for  $\alpha\Lambda\Lambda$ , and the Yakubovsky equations for  $\alpha\alpha\Lambda\Lambda$ , using model ESC00, as function of the number of terms  $N$  retained in the expansion (22). A cutoff radius  $R_{\text{cutoff}} = 19$  fm was used in both calculations.

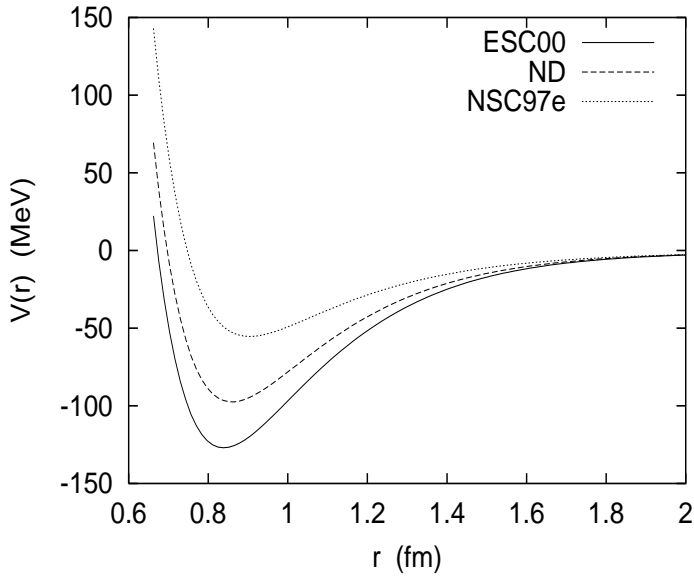


FIG. 2.  $\Lambda\Lambda$  potentials for various simulations of Nijmegen models.

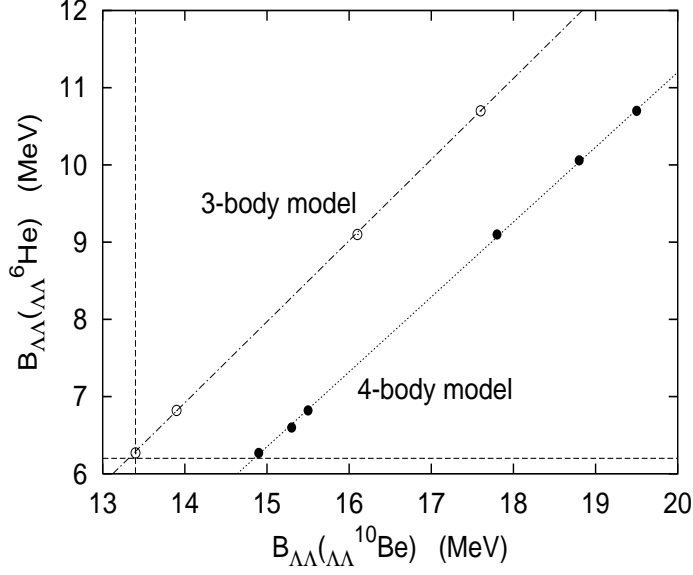


FIG. 3. Calculated binding energies  $B_{\Lambda\Lambda}$  for  ${}_{\Lambda\Lambda}^6\text{He}$  in a three-body  $\alpha\Lambda\Lambda$  model, and for  ${}_{\Lambda\Lambda}^{10}\text{Be}$  in a four-body  $\alpha\alpha\Lambda\Lambda$  model and in a three-body  ${}^8\text{Be}\Lambda\Lambda$  model.

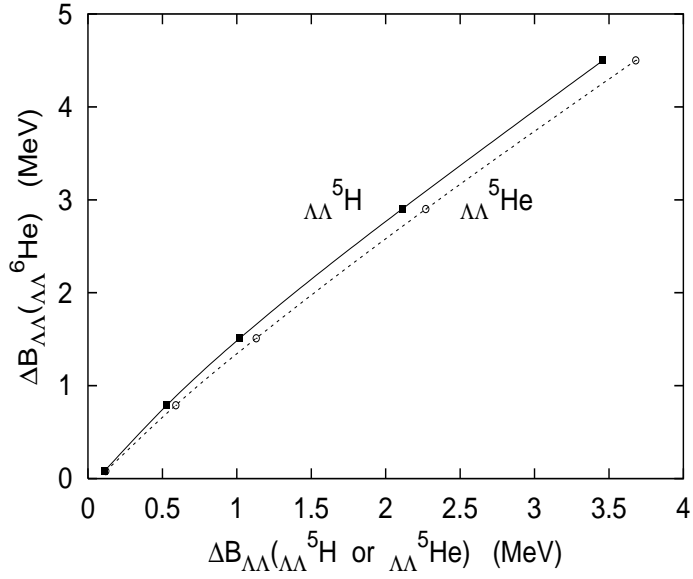


FIG. 4. Incremental binding energies  $\Delta B_{\Lambda\Lambda}$  calculated for  $A = 5, 6$  in a three-body model.  $\Delta B_{\Lambda\Lambda}(A=5)$  is relative to the  $(2J+1)$  average of the  $({}^4_{\Lambda}\text{H}, {}^4_{\Lambda}\text{He})$  levels of Table IV.